Tellus (1978), *30*, 468–471

SHORT CONTRIBUTION

Instability of a two-layer baroclinic flow in a channel

By C. R. CARRIGAN, *Department of Geodesy and Geophysics, Cambridge University, Cambridge, England CB3 0EZ*

(Manuscript received February 7; in final form May 29, 1978)

1. Introduction

The properties of the two-layer model for disturbances of a rotating baroclinic basic state have been investigated extensively over the last few decades by application of numerical and analytical techniques. Many of the studies, e.g., Pedlosky (1964a, b) and Drazin (1970), have assumed the presence of vertical sidewalls in the analysis for the purpose of supplying horizontal boundary conditions for the eigenfunction representing the disturbance. While Hart (1972) has considered in detail the linear and finite amplitude nature of baroclinic waves in a cylindrical tank, to the author's knowledge no experimental two-layer study which includes horizontal confinement has been presented in the literature. The present investigation uses the channel model as a basis for studying the stability of the axisymmetric regime over a wide range of reciprocal Burger number (F) and Rossby number (Ro) which represent a measure of the rotation rate of the system and the vertical shear of the axisymmetric regime respectively. The results are assessed using a linear theory which assumes a simple axisymmetric basic state. Additionally they are compared to Pedlosky's analysis (1964b) which considers the effects of horizontal shear on the stability of the basic state.

2. Linear equations

Fig. 1 is a cross section of the model which consists of two layers of fluid of differing but constant density ($\rho_1 < \rho_2$) confined to a channel undergoing rotation. The layers have velocities u_1 and u_2 which are constant and measured with respect to the rotating system. For systems characterized by geostrophic balance, tilting of the fluid interface with respect to potential surfaces occurs. This baroclinicity represents a source of available potential energy for disturbances which can overcome the dynamical constraints associated with rotation.

The linear perturbation vorticity equations for each layer in cylindrical coordinates have the non-dimensional form (Hart, 1972):

$$\left\{\frac{\partial}{\partial t} + u_1 \frac{\partial}{\partial \theta}\right\} \left\{\nabla^2 p_1 + F(p_2 - p_1)\right\} + \frac{\partial p_1}{\partial \theta}\left[\frac{-F}{4Ro}\cdot\frac{\Delta\rho}{\rho} + F(u_1 - u_2)\right] + \frac{E_1^{\frac{1}{2}}}{\sqrt{2}Ro} \times \left(\frac{1+2\chi}{1+\chi}\right)\cdot\nabla^2 p_1 - \frac{E_1^{\frac{1}{2}}}{\sqrt{2}Ro}\cdot\left(\frac{\chi}{1+\chi}\right)\cdot\nabla^2 p_2 = 0$$

$$\left\{\frac{\partial}{\partial t} + u_2 \frac{\partial}{\partial \theta}\right\} \left\{\nabla^2 p_1 + F(p_2 - p_1)\right\} + \frac{\partial p_2}{\partial \theta}\left[\frac{F}{4Ro}\cdot\frac{\Delta\rho}{\rho} - F(u_1 - u_2)\right] + \frac{E_2^{\frac{1}{2}}}{\sqrt{2}Ro} \times \left(\frac{2+\chi}{1+\chi}\right)\cdot\nabla^2 p_2 - \frac{E_2^{\frac{1}{2}}}{\sqrt{2}Ro}\cdot\left(\frac{\chi \Rightarrow 1}{1+\chi}\right)\cdot\nabla^2 p_1 = 0$$

where the $p_{1,2}$ are the perturbation streamfunctions for the two layers, ∇^2 is the horizontal Laplacian and the non-dimensional parameters are given by

$$F = 4\Omega^2 L^2/g \frac{\Delta\rho}{\rho} H$$

$$Ro = \omega/2\Omega$$

$$E_{1,2} = \nu_{1,2}/2\Omega H^2 \quad \text{and}$$

$$\chi = (\nu_2/\nu_1)^{1/2}.$$

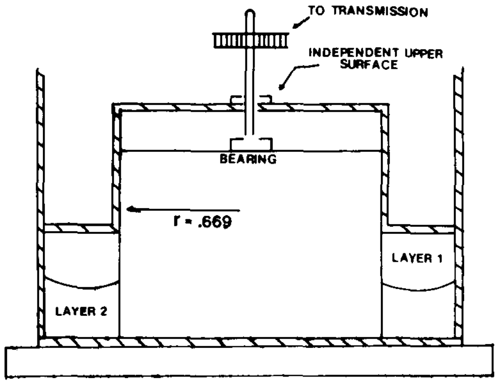

Fig. 1. Cross section of experimental apparatus showing two-layer channel geometry. The top boundary rotates independently of the table providing the shear required to produce baroclinicity.

L, H and ω represent the radius of the system used as the horizontal length scale, the depth of a layer used as the vertical length scale and the differential rotation rate of the top boundary of the experiment. Besides including terms for centrifugal and baroclinic effects (quantities in square brackets), the vorticity equations also include contributions of order $E^{1/2}$ due to a vertical suction resulting from the presence of Ekman boundary layers at the top, interface and bottom of the system. All these terms contribute to the critical shear cutoff which is manifested by the bending of the neutral stability curves in the F, $1/Ro$ plane (see Fig. 3).

Using Bessel functions of the first and second kind, a solution for the system was assumed to have the form:

$$p_{1,2} = [J_n(rl) \cdot Y_n(l) - J_n(l) \cdot Y_n(rl)]\, e^{in(\theta - ct)}$$

in which the azimuthal wavenumber is given by n and the complex phase speed by c. Substitution of this solution for p_1 and p_2 allows the partial differential equations to be reduced to a quadratic equation for c in terms of l, n, F and Ro. The solution satisfies the boundary condition, $p_{1,2} = 0$, at the outer wall, $r = 1$, identically, and a program was used to calculate the values of $l(n, r_i)$ which cause p to vanish at the inner wall, $r_i = 0.669$. Thus for a particular value of n, the quadratic equation may be used to calculate a neutral stability curve as a function of F and Ro.

3. The experiment

The setup (Fig. 1) consists of a perspex annulus 0.46 m in diameter, 0.30 m in height with a 0.0762 m gap which contains the working fluids. The annulus was centred on a high inertia turntable which allowed maintenance of a preset rotation rate to within 0.1%. The independently rotating top surface which is in contact with layer 1 provides the required shear (ω, the top rotation rate, is measured with respect to the table). Silicone oil having a density of 0.923 mg m^{-3} and kinematic

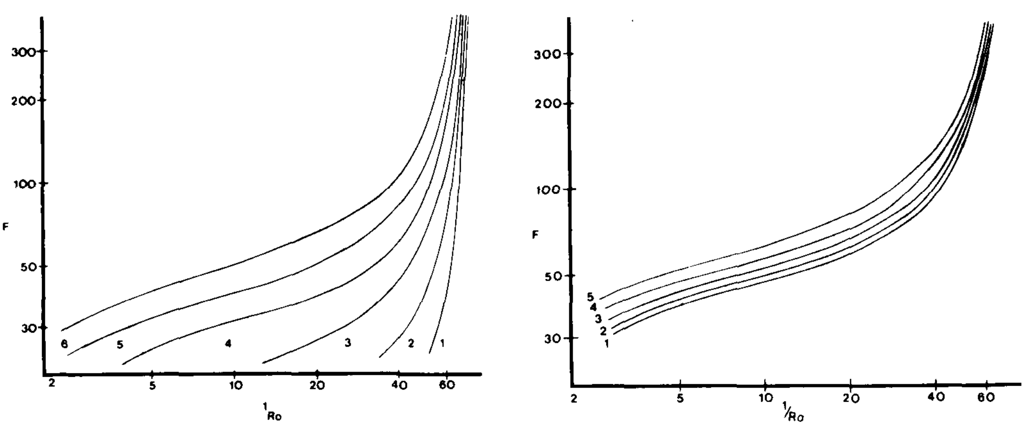

Fig. 2. Neutral stability curves for the unconfined (a) and $r = 0.669$ (b) cases without Ekman effects. F and $1/Ro$ represent a measure of the table rotation rate of the system and the vertical shear respectively. The mean rotation rate of the layers is used in calculating all curves.

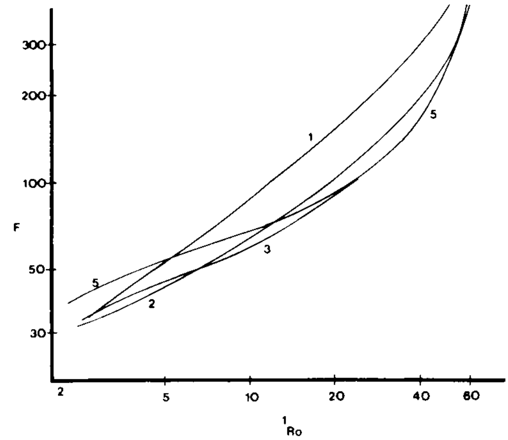

Fig. 3. Neutral stability curves for $r = 0.669$ with Ekman suction included. For increasing values of F, successively higher azimuthal modes are most unstable. ($n = 4$ not shown.)

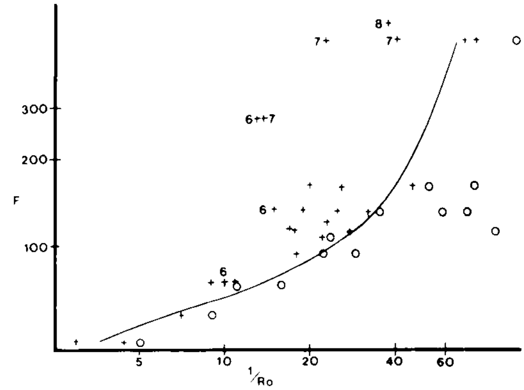

Fig. 4. Comparison between experimental data and calculated neutral curve for $n = 5$. Observation of instability is denoted by (+) and its absence by (O). Modes are $n = 5$ unless otherwise noted.

viscosity of 0.27 St was used for the lower layer while a water–methyl alcohol mixture comprised the upper layer which was characterized by density and kinematic viscosity values of 0.898 mg m^{-3} and 0.023 St respectively. The layers, each 0.051 m thick, were separated by an immiscible interface for which surface tension effects were minimized by the addition of a small amount of isopropyl alcohol. The viscosities ν_1 and ν_2, imply non-dimensional differential rotation rates for layers 1 and 2 of $U_1 = 0.61$ and $U_2 = 0.11$ calculated from a balance of the momentum flux across the Ekman layers. The instability appeared as a periodic deformation of the interface for which observations of wavenumber and onset as a function of F and Ro were obtained visually.

4. Results and conclusion

Figs. 2a and b provide a comparison of the effects of narrowing the channel on the neutral stability curves for different azimuthal wavenumbers as plotted in the F, $1/Ro$ plane. Terms involving Ekman suction have not been included. The most striking feature distinguishing the unconfined (2a) and the $r = 0.669$ case (2b) is the increased density of modes in the F, $1/Ro$ plane associated with the channel geometry. It should be noted, however, that only the mode density changes and the mode of instability associated with the lowest value of shear for a given value of F is still $n = 1$. Hart did observe this mode for the unconfined case when critical shear was achieved.

Fig. 3 illustrates the neutral stability curves for the channel when Ekman terms are included. Modes 2–5 are almost degenerate for small Ro and $n = 1$ is shifted above the others in contrast to Fig. 2b. Fig. 4 provides a comparison between the experiment and theory. Unstable modes (+) were usually observed to be $n = 5$ though higher modes occurred for higher shears and rotation rates as is expected. When the system was observed to be stable (O), the shear was slowly increased until instability was observed. The neutral curve for $n = 5$ (Ekman effects included) is plotted for reference. The neutral stability theory with Ekman suction predicts the position of the instability in the F, $1/Ro$ plane to within 10% except in the region of the critical shear cutoff where the observed destabilization may be caused by interior viscous diffusion. Unfortunately, agreement between the data and theory concerning the most unstable mode is not as straightforward. One might expect that for close lying modes, a small drift from the preset rotation and shear might be sufficient to excite several modes and cause $n = 5$ to dominate as a consequence of having the highest linear growth rate. Alternatively, Pedlosky (1964b) has demonstrated that horizontal shear in the basic state can shift the most unstable mode from a lower value of n to a higher one without changing the critical value of shear required for instability at a given F. That the sidewall boundary layers which scale as $E^{1/4}$ occupy about 20% of the gap width suggests that horizontal shear may be significant as a destabilizing mechanism for the higher modes which are observed in the experiment. From a comparison of Figs. 3 and 4, it is apparent that the higher mode data lies near the neutral stability curves for lower wavenumber–lower critical shear modes which is consistent with Pedlosky's results.

In conclusion the experiment indicates that linear theory with Ekman layers included represents a good estimate of the onset of instability in a rotating channel over a relatively wide range of F and Ro. For higher values of F the $n = 5$ mode was observed to dominate as predicted by the theory. However, for smaller values of F and higher values of shear ($1/Ro \to 0$) lower modes than $n = 5$ were expected though usually not observed. Destabilization of higher modes due to the presence of horizontal shear in the basic state could well account for such a result.

5. Acknowledgements

It is a pleasure to acknowledge Professor F. H. Busse for his support during this research. The major part of this work was carried out at the University of California, Los Angeles, with support from NSF Grant GA-41750. Funding at Cambridge was supplied by the NERC.

REFERENCES

Drazin, P. G. 1970. Non-linear baroclinic instability of a continuous zonal flow. *Quart. J.R. Met. Soc. 96*, 667–676.

Hart, J. E. 1972. A laboratory study of baroclinic instability. *Geophysical Fluid Dynamics 3*, 181–209.

Pedlosky, J. 1964a. The stability of currents in the atmosphere and the ocean, Part I. *J. Atmos. Sci. 21*, 201–219.

Pedlosky, J. 1964b. The stability of currents in the atmosphere and the ocean, Part II. *J. Atmos. Sci. 21*, 342–353.